



Published in final edited form as:

*Wound Repair Regen.* 2019 November ; 27(6): 711–714. doi:10.1111/wrr.12758.

## Characterizing Differences in the Collagen Fiber Organization of Skin Wounds Using Quantitative Polarized Light Imaging

Alan E. Woessner<sup>†</sup>, James D. McGee<sup>†</sup>, Jake D. Jones, Kyle P. Quinn<sup>\*</sup>

Department of Biomedical Engineering, University of Arkansas, Fayetteville, AR, USA

### Abstract

Collagen fiber organization requires characterization in many biomedical applications, but is difficult to objectively quantify in standard histology tissue sections. Quantitative polarized light imaging is a low-cost technique that allows for rapid measurement of collagen fiber orientation and thickness. In this study, we utilize a quantitative polarized light imaging system to characterize fiber orientation and thickness from wound sections. Full thickness skin wound sections that were previously stained with hematoxylin and eosin were used to assess collagen fiber content and organization at different points during the wound healing process. Overall, wounds exhibited a measurable increase in collagen fiber thickness and a nonlinear change in fiber reorganization within the wound. Our study demonstrates that quantitative polarized light imaging is an inexpensive alternative or supplement to standard histology protocols, requiring no additional stains or dyes, and yields repeatable quantitative assessments of collagen organization.

### Introduction

Assessing collagen in a skin wound and its adjacent dermis is critical to understanding the effect of disease and treatment on wound healing<sup>1-3</sup>. Standard techniques for visualizing collagen such as hematoxylin and eosin (H&E) and Masson's trichrome staining however yield qualitative information on collagen alignment and deposition. Polarized light imaging in combination with Picrosirius red staining to enhance the natural birefringence of collagen, has been used to observe collagen alignment in the dermis, but this analysis typically only provides categorical information on fiber thickness based on color interference and lacks fiber orientation data<sup>4</sup>. Quantitative polarized light imaging (QPLI) is a diffraction-limited imaging method that also exploits the natural birefringence of collagen to measure both pixel-wise collagen fiber orientation and fiber thickness based on light phase retardation<sup>5, 6</sup>. Previously, QPLI has been used in various biomedical applications, including the visualization of fiber organization surrounding tumors, mapping the brain connectome, and detecting fiber reorganization in ligaments during mechanical loading<sup>7-12</sup>. Here, we demonstrate the development of a cost effective and automated QPLI system and its

<sup>\*</sup> **Corresponding Author:** Kyle P. Quinn, Ph.D., Department of Biomedical Engineering, University of Arkansas, 123 John A. White Jr. Engineering Hall, Fayetteville, AR, 72701, USA, Tel: 479-575-5364, kyle@quinnlab.org.

<sup>†</sup> These authors have contributed equally to this work

*Conflict of Interest disclosure statement:* The authors have no conflicts of interest.

application to assessing the collagen organization of skin wounds from H&E stained sections.

## Methods

### QPLI System Overview

Quantitative polarized light imaging is achieved by outfitting imaging systems with a rotating linear polarizer and a fixed circular analyzer, in contrast to the standard crossed linear polarizer setup typically utilized in Picrosirius red staining. To implement QPLI with an existing upright Olympus BX51 microscope (Olympus; Tokyo, Japan), we first retrofitted it with a 660 nm LED light source and collimator (ThorLabs; Newton, NJ). A linear polarizer sheet (American Polarizers Inc.; Reading, PA) attached to a piece of thin acrylic was placed below the sub stage condenser lens and rotated by a stepper motor driven by a motor shield (Adafruit Industries; New York City, NY) and Arduino UNO (Figure 1A). Light that passes through the rotating polarizer, condenser lens, and sample is then collected with a 20x, 0.5 NA dry objective lens (Olympus; Tokyo, Japan). Light collected by the objective lens then passes through a circular analyzer that was constructed by placing the linear polarizer material at 45 degrees relative to a quarter-wave plate (165 nm, American Polarizers Inc.; Reading, PA). Finally, the light passes through a 660 nm bandpass filter (ThorLabs; Newton, NJ) and is collected with a camera (Lumenera Corp.; Ottawa, ON) (Figure 1A). To ensure that light intensity is not partially linearly polarized and independent of the rotating linear polarizer angle, a fixed right-handed circular polarizer was also placed below the rotating polarizer. During acquisition, images are collected as the linear polarizer rotates in increments of 18°, resulting in a set of 10 images (2056×2056 pixels; 0.294 mm per pixel). Image collection and analysis was automated using custom written MATLAB code (MathWorks; Natick, MA). Collagen fibers at each pixel will produce a sinusoidal oscillation of light intensity as the rotating polarizer spans 180° due to their linear birefringent properties (Figure 1C). The phase and amplitude of this oscillation is proportional to the fiber orientation and thickness, respectively<sup>6</sup> (Figure 1B,C).

### System Error

In order to minimize the amount of measurement error, correction factors to account for optical misalignment were calculated as previously described<sup>5</sup>. System error was then quantified using a wave plate with a known phase retardation and orientation (140 nm, American Polarizers Inc.; Reading, PA). QPLI data of the calibration wave plate were collected at various orientations, and absolute differences between theoretical to calculated orientation and retardation values yielded mean errors of  $1.78^\circ \pm 1.01$  and  $6.54^\circ \pm 1.78$ , respectively. Additionally, measurements of the background signal with no tissue sample exhibited a non-preferential orientation and a mean retardation error of  $0.69^\circ \pm 0.17$ .

### Sample Preparation

To demonstrate the utility of the system in wound healing research, a standard pre-clinical mouse model was used. All experiments were approved and performed according to the University of Arkansas IACUC (Protocol #16001). Full-thickness excisional wounds were created on the dorsum of both STZ-injected diabetic (n = 13) and control (n = 10) C57BL/6J

mice (12 weeks; male) using a sterile 6 mm biopsy punch. On either day 3, 5, or 10 post-wounding, approximately 1 cm<sup>2</sup> of skin surrounding the wound was excised from each mouse following euthanasia. All tissue samples, including the biopsied tissue at day 0, were frozen in OCT at -80°C. The frozen wound tissue were sectioned into 30 µm thick samples, transferred to glass slides, and stained with H&E<sup>13</sup>.

### Image Processing of Alignment and Retardation Maps

The collected intensity oscillation at each pixel is processed using a harmonic analysis algorithm to compute the relative phase and magnitude of the intensity response<sup>5, 6, 12</sup>. Briefly, the harmonic analysis algorithm computes only the first sine and cosine coefficients of a Fourier series. These coefficients are used to compute the relative magnitude and phase of the intensity oscillation for each pixel as a function of rotating linear polarizer orientation (Figure 1C). When a linear birefringent media is assumed, the pixel-wise fiber orientation is proportional to the phase of the intensity oscillation, and is exactly  $\pm 45^\circ$  off of the peak of the intensity oscillation, depending on the handedness of the circular analyzer. All pixel-wise fiber orientations are reported such that 0° corresponds to the horizontal axis of the image. Light retardation, which is a function of birefringence and fiber thickness, is proportional to the magnitude of the oscillation. After pixel-wise maps of fiber orientation and retardation are produced, intensity-based image correlation was used to determine relative image positions, and the maps are stitched together using a distance-weighted averaging approach<sup>14</sup>.

Dermis and wound regions of interest were manually traced in MATLAB. Based on the accuracy of retardation measurements in the image background, all pixels with a retardation value exceeding 2° within these regions defined as collagen-positive regions. In order to eliminate small structures associated with noise, the binary collagen-positive mask was opened with a 2-pixel radius disk. Directional statistics were used to determine the mean fiber orientation and directional variance within each ROI, and local directional variance and fiber density were mapped by summarizing the orientation distribution within a radius of 500 pixels at each pixel<sup>14</sup>. To evaluate differences, a nested ANOVA model with interactions (JMP Pro 13; Cary, NC) and post-hoc Tukey's HSD tests were used ( $\alpha = 0.05$ ).

## Results

QPLI-derived maps of collagen fiber organization revealed location-dependent differences in fiber alignment, fiber thickness, and collagen-positive pixel density over time (Figure 2). Within the wound bed, average light retardation and the fraction of collagen-positive pixels increased over time with a significant differences between days 3 and 10 ( $p < 0.0001$ ) (Figure 2G,H). This increase in fiber thickness and density detected within the wound bed by our QPLI system over 10 days demonstrates its sensitivity to the expected skin wound healing response. Additionally, there were dynamic changes in the fiber alignment within the wound over time (Figure 2F). A significant decrease in fiber directional variance from day 3 to 5 ( $p = 0.013$ ) indicated an increase in local fiber alignment. However by day 10, directional variance increased relative to day 5 ( $p=0.003$ ), indicating more randomly aligned organization.

No differences were detected between the fiber organization in diabetic and non-diabetic mice ( $p=0.692$ ). In the dermis adjacent to the wound, no significant differences were found with respect to the directional variance over time, indicating a consistent collagen network without a preferred fiber orientation (Figure 2F). A small decrease in the fraction of collagen-positive pixels in the adjacent dermis was observed on day 10 relative to day 0 ( $p < 0.0001$ ), and day 5 ( $p = 0.004$ ) (Figure 2H). A similar trend was observed in the light retardation measurements, with a significant decrease between day 0 and day 10 ( $p < 0.0001$ ) (Figure 2G). These findings suggest a decrease in fiber thickness and amount in the adjacent dermis during the wound healing process, which may be related to the active remodeling occurring in the wound or tissue deformation associated with wound contraction.

## Discussion

QPLI allows for the rapid and automated quantification of collagen fiber organization within skin wounds. The method yields continuous data on pixel-wise fiber orientation and light retardation, which is directly proportional to fiber thickness for thin samples. Picrosirius red staining and crossed linear polarizers are often used to assess fiber thickness through the light interference patterns produced by the enhanced collagen birefringence<sup>4</sup>. However, this colorimetric analysis of red, yellow, and green fibers only provides thickness measurements in discrete categories based on color. Additionally, crossed linear polarizer configurations cannot detect fibers that are aligned with either of the linear polarizer axes, resulting in potentially significant errors in fiber measurements. Crossed circular polarizers have been previously used to eliminate these fiber measurement errors; however, the fiber thickness measurements still rely on categorizing fibers based on colorimetric analysis<sup>15</sup>. QPLI utilizes a rotating linear polarizer element, which not only returns a continuous variable corresponding to fiber thickness, but also allows for accurate detection of fiber orientation at each pixel. Although algorithms have been previously developed to produce quantitative pixel-wise fiber orientation maps based on Masson's trichrome intensity, these methods lack the accuracy of QPLI ( $1.78^\circ$ ) or the ability to provide fiber thickness measurements<sup>14, 16</sup>. QPLI does not require any exogenous stains or dyes, but can also be done on previously stained samples as demonstrated here, potentially saving valuable tissue sections for additional analysis. Although  $30\ \mu\text{m}$  tissue sections were used in this study, the high accuracy of the system at low retardation values ( $0.69^\circ \pm 0.17$ ) indicates that this technique can be applied to a wide range of tissue thicknesses between  $4\text{-}50\ \mu\text{m}$ . With a total cost of roughly 300 USD to retrofit an existing microscope, this quantitative method is similar in cost to the reagents needed for most collagen staining protocols. In this study, we have demonstrated the application of QPLI to characterizing collagen organization in excisional wounds, however, it can easily be applied to other wound types or skin applications.

## Acknowledgements

*Source of funding:* This research was funded by NIH grant numbers R00EB017723 and R01AG056560, as well as the Arkansas Biosciences Institute.

## References

1. Connizzo BK, Bhatt PR, Liechty KW, Soslowsky LJ. Diabetes alters mechanical properties and collagen fiber re-alignment in multiple mouse tendons. *Ann Biomed Eng.* 2014;42(9):1880–8. [PubMed: 24833253]
2. Ehrlich HP, Hunt TK. Collagen Organization Critical Role in Wound Contraction. *Adv Wound Care (New Rochelle).* 2012;1(1):3–9. [PubMed: 24527271]
3. Xue M, Jackson CJ. Extracellular Matrix Reorganization During Wound Healing and Its Impact on Abnormal Scarring. *Adv Wound Care (New Rochelle).* 2015;4(3):119–36. [PubMed: 25785236]
4. Lattouf R, Younes R, Lutomski D, Naaman N, Godeau G, Senni K, et al. Picrosirius red staining: a useful tool to appraise collagen networks in normal and pathological tissues. *J Histochem Cytochem.* 2014;62(10):751–8. [PubMed: 25023614]
5. Tower TT, Neidert MR, Tranquillo RT. Fiber Alignment Imaging During Mechanical Testing of Soft Tissues. *Ann Biomed Eng.* 2002;30:1221–33. [PubMed: 12540198]
6. Glazer AM, Lewis JG, Kaminsky W. An Automatic Optical Imaging System for Birefringent Media. *Proc R Soc Lond A.* 1996;452:2751–65.
7. Axer M, Amunts K, Grassel D, Palm C, Dammers J, Axer H, et al. A novel approach to the human connectome: ultra-high resolution mapping of fiber tracts in the brain. *Neuroimage.* 2011;54(2):1091–101. [PubMed: 20832489]
8. Axer M, Grassel D, Kleiner M, Dammers J, Dickscheid T, Reckfort J, et al. High-resolution fiber tract reconstruction in the human brain by means of three-dimensional polarized light imaging. *Front Neuroinform.* 2011;5:34. [PubMed: 22232597]
9. Keikhosravi A, Liu Y, Drifka C, Woo KM, Verma A, Oldenbourg R, et al. Quantification of collagen organization in histopathology samples using liquid crystal based polarization microscopy. *Biomed Opt Express.* 2017;8(9):4243–56. [PubMed: 28966862]
10. Komatsu K, Mosekilde L, Viidik A, Chiba M. Polarized light microscopic analyses of collagen fibers in the rat incisor periodontal ligament in relation to areas, regions, and ages. *Anat Rec.* 2002;268(4):381–7. [PubMed: 12420286]
11. Quinn KP, Winkelstein BA. Vector correlation technique for pixel-wise detection of collagen fiber realignment during injurious tensile loading. *J Biomed Opt.* 2009;14(5):054010. [PubMed: 19895112]
12. Quinn KP, Winkelstein BA. Altered collagen fiber kinematics define the onset of localized ligament damage during loading. *J Appl Physiol (1985).* 2008;105(6):1881–8. [PubMed: 18845780]
13. Jones JD, Ramser HE, Woessner AE, Quinn KP. In vivo multiphoton microscopy detects longitudinal metabolic changes associated with delayed skin wound healing. *Commun Biol.* 2018;1:198. [PubMed: 30480099]
14. Quinn KP, Golberg A, Broelsch GF, Khan S, Villiger M, Bouma B, et al. An automated image processing method to quantify collagen fibre organization within cutaneous scar tissue. *Exp Dermatol.* 2015;24(1):78–80. [PubMed: 25256009]
15. Whittaker P, Kloner RA, Boughner DR, Pickering JG. Quantitative assessment of myocardial collagen with picrosirius red staining and circularly polarized light. *Basic Res Cardiol.* 1994;89(5):397–410. [PubMed: 7535519]
16. Quinn KP, Georgakoudi I. Rapid quantification of pixel-wise fiber orientation data in micrographs. *J Biomed Opt.* 2013;18(4):046003. [PubMed: 23552635]

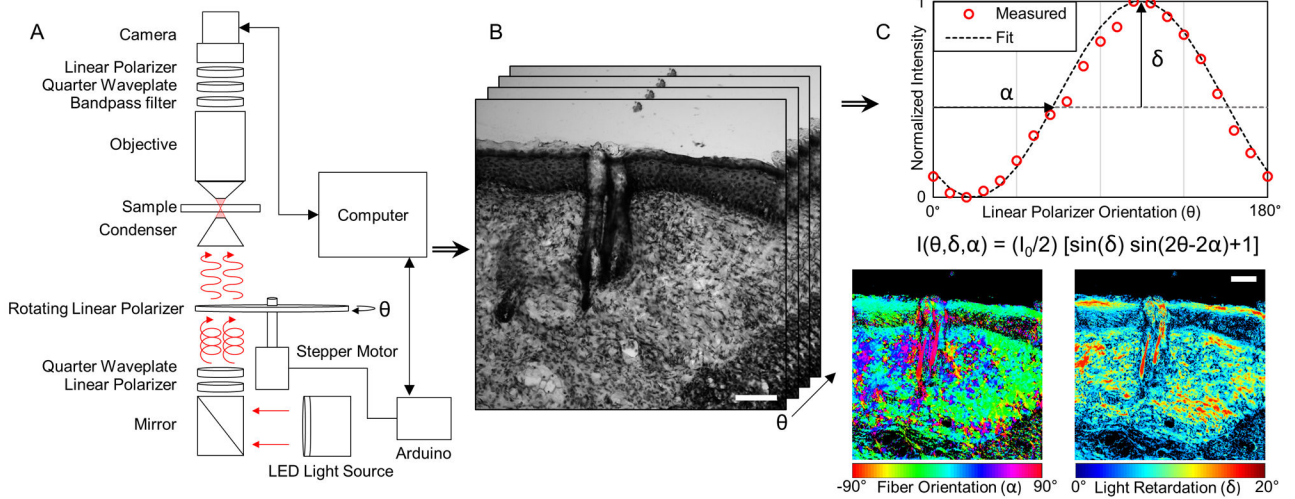


**Figure 1.** Summary of QPLI acquisition and analysis for measuring fiber orientation thickness. (A) Light from a 660nm LED (red arrows) becomes circularly polarized by a linear polarizer and quarter-wave plate before passing through a rotating linear polarizer. The linear polarized light at an angle ( $\theta$ ) defined by a stepper motor is focused onto collagenous sample that alters the polarization state. A bandpass filter, quarter-wave plate and linear polarizer act as a circular analyzer, converting the 660nm light back to linear polarization before collection by the camera. (B) A set of 10 intensity images are acquired at different polarization angles,  $\theta$ . (C) The phase and amplitude of light intensity oscillation at any pixel as the polarizer angle,  $\theta$ , rotates is used to compute fiber orientation ( $\alpha$ ) and light retardation ( $\delta$ ), respectively. By assuming the collagen sample at each pixel is linear birefringent, pixel-wise orientation and retardation maps can be generated. Orientation maps are color-coded such that  $0^\circ$  corresponds to the horizontal axis of the image. Scale bars represent  $100 \mu\text{m}$ .

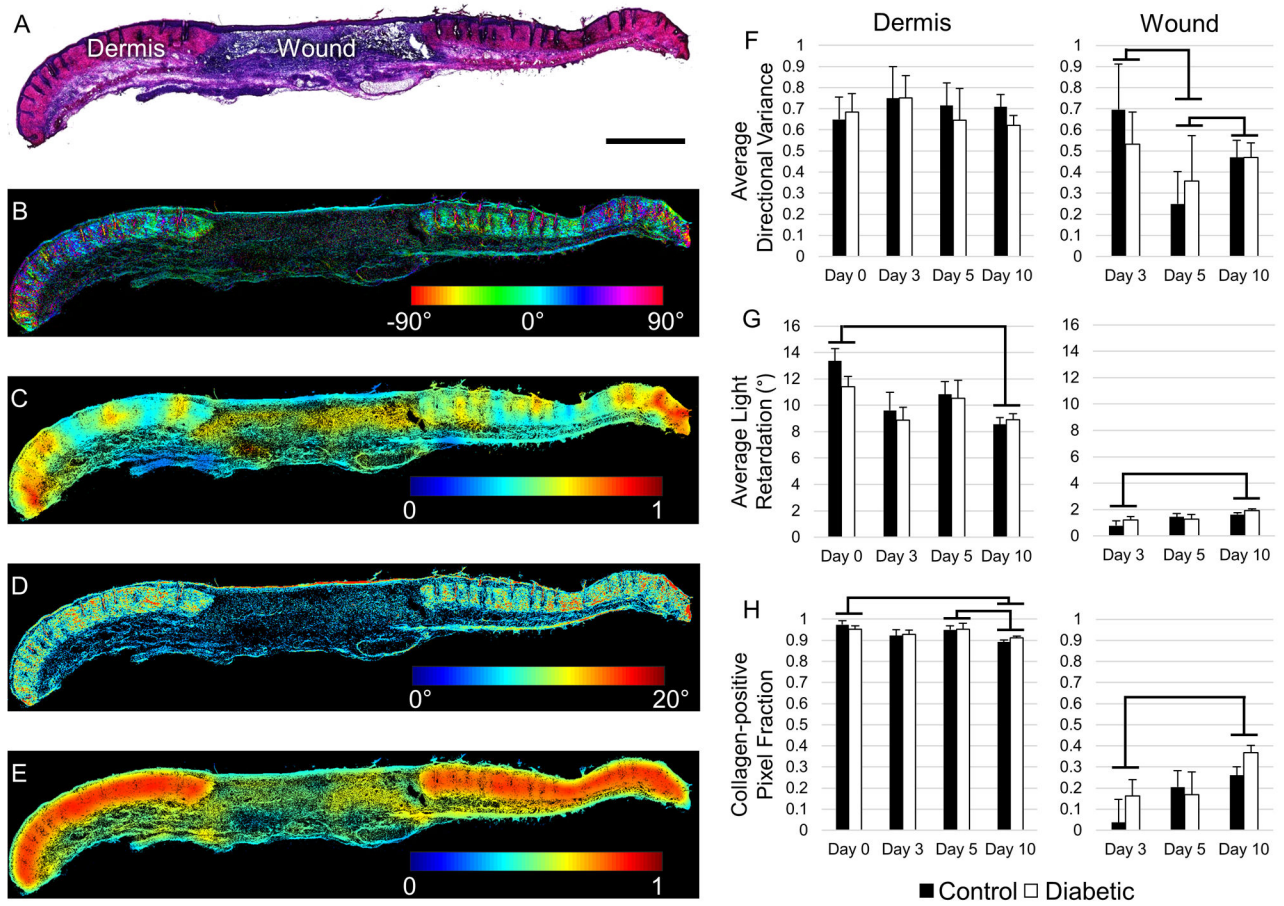


**Figure 2.** Quantitative analysis of collagen fiber organization in excisional wound sections. (A) A representative H&E stained tissue section containing both the wound site and adjacent dermis at day 10 post-wounding. Scale bar represents 100  $\mu\text{m}$ . (B) QPLI-derived collagen fiber orientation map.  $0^\circ$  corresponds to the horizontal axis of the image. (C) Map of local fiber directional variance within a 500 pixel radius. (D) QPLI-derived phase retardation map indicating fiber thickness. (E) A map of local collagen fiber density, based on collagen positive pixels within a 500 pixel radius. (F-H) Average directional variance, light retardation, and collagen-positive pixel count fraction for the adjacent dermis (left column) and wound bed (right column), respectively. All error bars represent standard error. Significance bars represent comparisons where  $p < 0.05$ .